Land surface - atmosphere coupling strength in the Hadley Centre GCM: the impact of soil physics

P.L. Vidale[1], A. Verhoef[2], M.E. Demory[1] and M.Roberts[3]

[1] NCAS-Climate, Meteorology Building, University of Reading, PO Box 243, Reading RG6 6BB, UK, e-mail: p.l.vidale@reading.ac.uk

[2] Department of Soil Science, School of Human and Environmental Sciences, The University of Reading, Reading RG6 6DW, UK, e-mail: a.verhoef@reading.ac.uk

[3] Meteorological Office, Exter, United Kingdom.

Summary

The introduction of a more realistic treatment of soil physics (corrected hydraulic parameters, improved parameterisation of thermal conductivity) in the Hadley Centre GCM (HadGAM1) profoundly affects soil water and thermal dynamics, as well as plant activity. These changes are particularly noteworthy at high latitudes, where the enhanced heat transfer in the soil alters the fraction of unfrozen water, which is made available to plant roots and activates Gross Primary Productivity (GPP), enabling longer-lasting growing seasons and enhanced seasonal to interannual variability. Furthermore, monthly soil moisture versus 1.5 m temperature anomalies suggest a stronger land surface-atmosphere coupling after parameter correction, in particular when both hydraulic parameters and the soil thermal conductivity formulation are updated. Soil physics improvements and related research on land surface processes promise to increase the level of coupling in Hadley Centre GCMs, enabling a larger role in the hydrological cycle for plant transpiration, with longer memory; however, the entire carbon cycle may need to be re-tuned.

1. Introduction

Understanding the land surface component of the hydrological cycle has been a high priority for decades. The routing of water through the soil-vegetation system is crucial to our understanding of the water-carbon cycles, as well as for the simulation of floods and droughts. The lack of global, homogeneous data regarding soil moisture amount and variability makes it difficult to close this gap and the use of numerical models is unavoidable. The land-atmosphere coupling strength in GCMs has been under scrutiny in the last few years, due to its role in closing the hydrological cycle at several time scales, which it modulates via memories in the terrestrial water balance (see e.g. Koster et al., 2002). Model intercomparison studies have indicated that there is no consensus on the correct magnitude of the coupling strength and several hypotheses to explain the disagreement have been raised, involving precipitation frequency/intensity characteristics, soil processes (infiltration, runoff generation, root extraction), and boundary layer dynamics. When simulating climate and its variability it is therefore important to assess the impact of the uncertainty in the treatment of soil prognostics (moisture and temperature), which stems from physical parameterizations, numerical discretisation and parameters This study addresses principally the sensitivity of key land surface and soil variables, as well land surface fluxes, to soil hydraulic parameters, as well as to the formulation of soil thermal conductivity, in the Hadley Centre GCM (HadGAM1).

2. Materials and Methods

2.1. Soil hydraulics

A historic error in the parameterisation of the water retention curve in the Met Office land surface models (MOSES and JULES) has been found recently (see also Dharssi et al., 2009). The soil hydraulic parameters that control the vertical flux of soil water (ψ_s and K_s) had been miscalculated by mis-interpreting a base-10 logarithm for a natural logarithm in Cosby et al.'s (1984) paper. This error affects matric potential (suction):

$$\psi = \psi_s \left(\frac{\theta}{\theta_s} \right)^{-b} \tag{1}$$

where ψ_s is the matric potential at saturation (m), θ is the soil moisture content ($m^3\ m^{-3}$) and θ_s the saturated soil moisture content ($m^3\ m^{-3}$). Parameter b (unitless) denotes the slope of the water retention curve. Furthermore, hydraulic conductivity

$$K = K_s \left(\frac{\theta}{\theta_s} \right)^{2b+3} \tag{2}$$

is also affected. Here, K_s is the saturated hydraulic conductivity ($m\ s^{-1}$).

A change in ψ_s also influences the soil moisture thresholds that control vegetation water stress and soil evaporation, via the moisture availability function, β, and the soil conductance for evaporation, g_{soil}:

$$\beta = \begin{cases} 1 \\ \dfrac{\theta - \theta_w}{\theta_c - \theta_w} \\ 0 \end{cases} \tag{3}$$

$$g_{soil} = \frac{1}{100} \left(\frac{\theta_1}{\theta_c} \right)^2 \tag{4}$$

Here θ_1 is the soil moisture content of the first layer. β also affects photosynthesis and hence GPP.

Table 1 below and Figures 1 and 2 illustrate the consequences of this error for FLUXNET sites that span a typical range of soil types (see also Verhoef and Vidale, 2009).

2.2. Soil thermal transfer

The parameterisation of thermal conductivity in the soil has also been updated, using a recent formulation by Lu et al. (2007), with some modifications. The thermal conductivity is calculated using:

$$\lambda = (\lambda_{\text{sat}} - \lambda_{\text{dry}}) K_{\text{e}} + \lambda_{\text{dry}} \tag{5}$$

where K_e is the Kersten number as given by

$$K_{\text{e}} = \exp\left\{ \alpha \left[1 - S_r^{\alpha - 1.33} \right] \right\} \tag{6}$$

Table 1. Soil hydraulic parameters and related soil moisture tresholds, values in bold indicate the corrected hydraulic parameterisation. The soil textural information at the FLUXNET sites given below has been obtained from the 5' IGBP-DIS soil texture data, aggregated onto the 135km GCM grid. Hence, these data were not obtained from the FLUXNET information websites. This decision was made so as to allow for a consistent comparison between the 1-D offline JULES runs (see Verhoef and Vidale, 2009) and those with the HadGAM1 GCM. El Saler exhibits the highest sand content and is classified as a sandy loam. The heaviest soil texture is the one obtained from finding the nearest gridbox to the Bondville coordinates: a clay loam, whereas Boreas-NSA is classified as a loamy soil.

Site	ψ_s [m]	K_s [mm s^{-1}]	θ_c [m^3 m^{-3}]	θ_w [m^3 m^{-3}]	θ_c-θ_w [m^3 m^{-3}]
El Saler	0.026/**0.089**	0.0086/**0.0109**	0.164/**0.206**	0.082/**0.103**	0.083/**0.103**
Boreas_NSA	0.043/**0.288**	0.0052/**0.0034**	0.238/**0.314**	0.137/**0.181**	0.101/**0.133**
Bondville	0.038/**0.217**	0.0051/**0.0033**	0.257/**0.316**	0.163/**0.201**	0.094/**0.115**

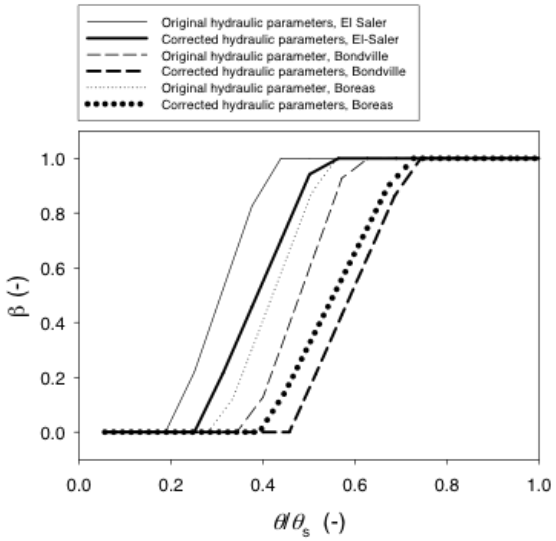

Figure 1. The soil moisture availability factor, β, for El Saler, Spain (solid lines), Boreas, Canada (dashed lines) and Bondville, USA (dotted lines) soils as a function of relative saturation before (standard thickness line) and after correction (thick line) of ψ_s (moving from a ln-based PTF to a ^{10}log-based PTF).

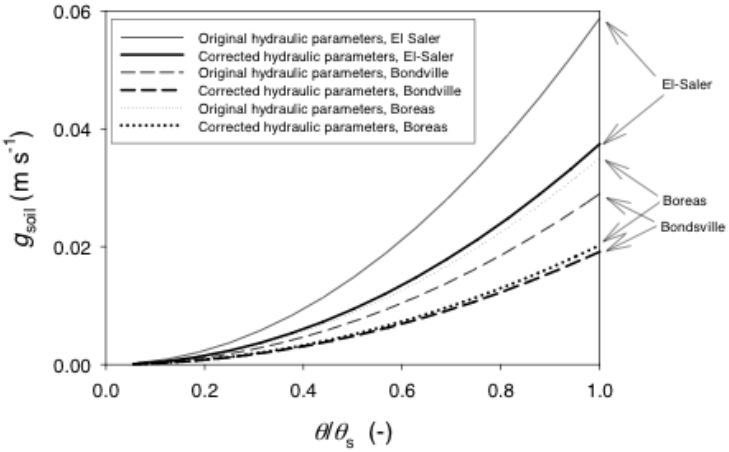

Figure 2. As in Fig. 1, but in this case showing g_{soil}, the soil conductance for evaporation (m s^{-1}).

where $S_r = \theta/\theta_s$. In Eq. 6, α is a soil-texture dependent parameter ($\alpha = 0.96$ for coarse-textured soils, i.e. with $f_{sand} > 0.40$, and $\alpha = 0.27$ for medium to fine-textured soils, i.e. with $f_{sand} < 0.40$) and 1.33 is a shape parameter. For frozen soils we have assumed $K_e = S_r$ as is the case in the JULES equations for thermal conductivity.

Lu et al. (2007) propose a linear equation for the calculation of λ_{dry}:

$$\lambda_{dry} = a\theta_s + b \tag{7}$$

Eq. 7 fits the heat pulse-based thermal conductivity data taken from the work by Johansen (1975) and Lu et al. (2007) slightly better than the equation proposed by Johansen (1975). Constants a and b were found to be -0.56 and 0.51, respectively.

Saturated thermal conductivity is estimated using

$$\lambda_{sat} = \lambda_s^{(1-\theta_s)} \lambda_w^{x_u} \lambda_i^{\theta_s - x_u} \tag{8}$$

with λ_w and λ_i the thermal conductivity of water and ice, respectively. Parameter λ_s is the thermal conductivity of the soil solids which is found from

$$\lambda_s = \lambda_q^{QC} \lambda_o^{1-QC} \tag{9}$$

Here QC is the quartz content (taken as the sand fraction, and ranging between 0-1), λ_q the thermal conductivity of quartz (7.7 W m^{-1} K^{-1}) and λ_o the thermal conductivity of other minerals (2.0 W m^{-1}K^{-1} for $QC > 0.2$ and 3.0 W m^{-1} K^{-1} otherwise). Variable x_u in Eq. 8 is the unfrozen volume fraction $= (\theta_s \frac{S_u}{S_u + S_f})$, with S_u and S_f the relative saturation for unfrozen $(S_u = \frac{\theta_u}{\theta_s})$ and frozen $(S_f = \frac{\theta_f}{\theta_s})$ water, respectively. For more details, the reader is referred to Verhoef and Vidale (2009).

Figure 3 shows how the new parameterisation produces larger, more realistic, values of thermal conductivity, especially for saturated soils in frozen conditions. This thermal behaviour and its interplay with soil water dynamics, profoundly affects plant activity and evaporation.

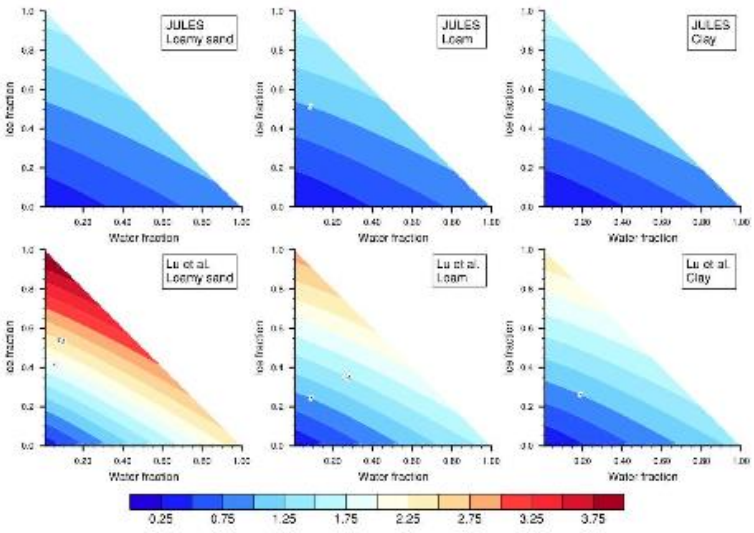

Figure 3. Thermal conductivity as a function of water and ice fraction, calculated using the standard JULES/MOSES parame-terisation (top panels) and with the parameterisation given in Lu et al. (2007), bottom panels, for three different soil types (sandy loam, loam and clay).

2.3. GCM Model runs

Model experiments focussed on the effect of corrected soil hydraulic parameter sets and the additional influence of an improved parameterisation for thermal conductivity. Sensitivity runs were performed entailing the following configurations:

CTL (bold line): Original MOSES hydraulic parameters and thermal parameterisation, using the standard Wilson Henderson-Sellers soil map as employed by UK Meteorological Office (UKMO) to provide sand/silt/clay content.

REF (map) (black line): Original MOSES hydraulic parameters and thermal parameterisation, but in this case with the soil map changed to IGBP-DIS.

Hyd (dashed line): Updated MOSES hydraulic parameters and original thermal parameterisation; IGBP-DIS soil map.

λ-Hyd (dotted line): Updated MOSES hydraulic parameters as well as thermal parameterisation; IGBP-DIS soil map.

3. Results

3.1. Results from GCM point extractions at FLUXNET sites

Simulations of the impact of soil physics at individual locations around the globe (see also Verhoef and Vidale, 2009), using GCM meteorological forcing, reveal the strong interplay between soil dynamics and plant activity, with significant reductions in GPP at locations where water extraction is hindered after correcting for the error in the computation of hydraulic parameters. In cold climates, the impact of increased thermal conductivity is well visible at depth, where more liquid water is available in the growing season.

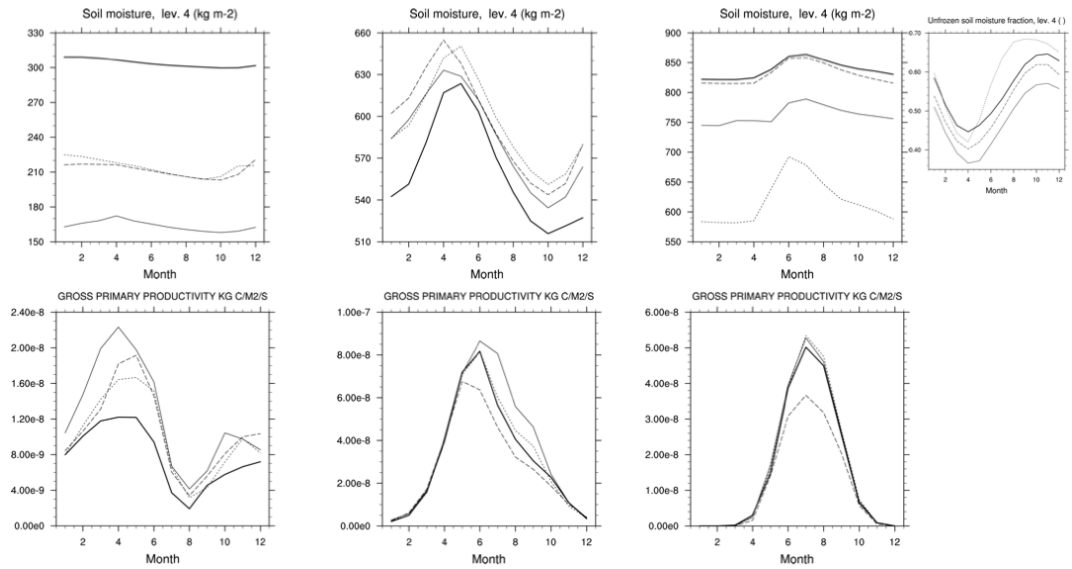

Figure 4. Level 4 (deepest soil layer) soil moisture content and GPP at selected FLUXNET sites worldwide: El Saler (Spain), Bondville (USA), Boreas–NSA (Canada). These figures involve extractions from the GCM runs around the sites' coordinates (9 nearest gridboxes). The four lines represent the different simulations detailed in Section 2.3.

3.2. Global maps of GCM simulations and regional seasonal evolution

The global maps of latent heat flux and GPP, as well as seasonal cycles of the regional evolution of key surface and sub-surface variables, reveal a chain of mechanisms that is consistent with the results from the single-site simulations: a change in the definition of mineral composition (see Table 1) has mostly a minor impact, except locally over small areas in which a large change in mineral content is imposed. Correcting the soil hydraulic parameters to the log-10 formulation depresses latent heat fluxes from the surface during the growing seasons, as well as vegetation production. Updating the parameterisation of soil thermal conductivity makes it possible to increase soil heat flux, e.g. to melt deep soil water at high latitudes, enhancing deep drainage, but also partially restoring the deficit in plant photosynthetic activity, through increased liquid water ratio in the soil.

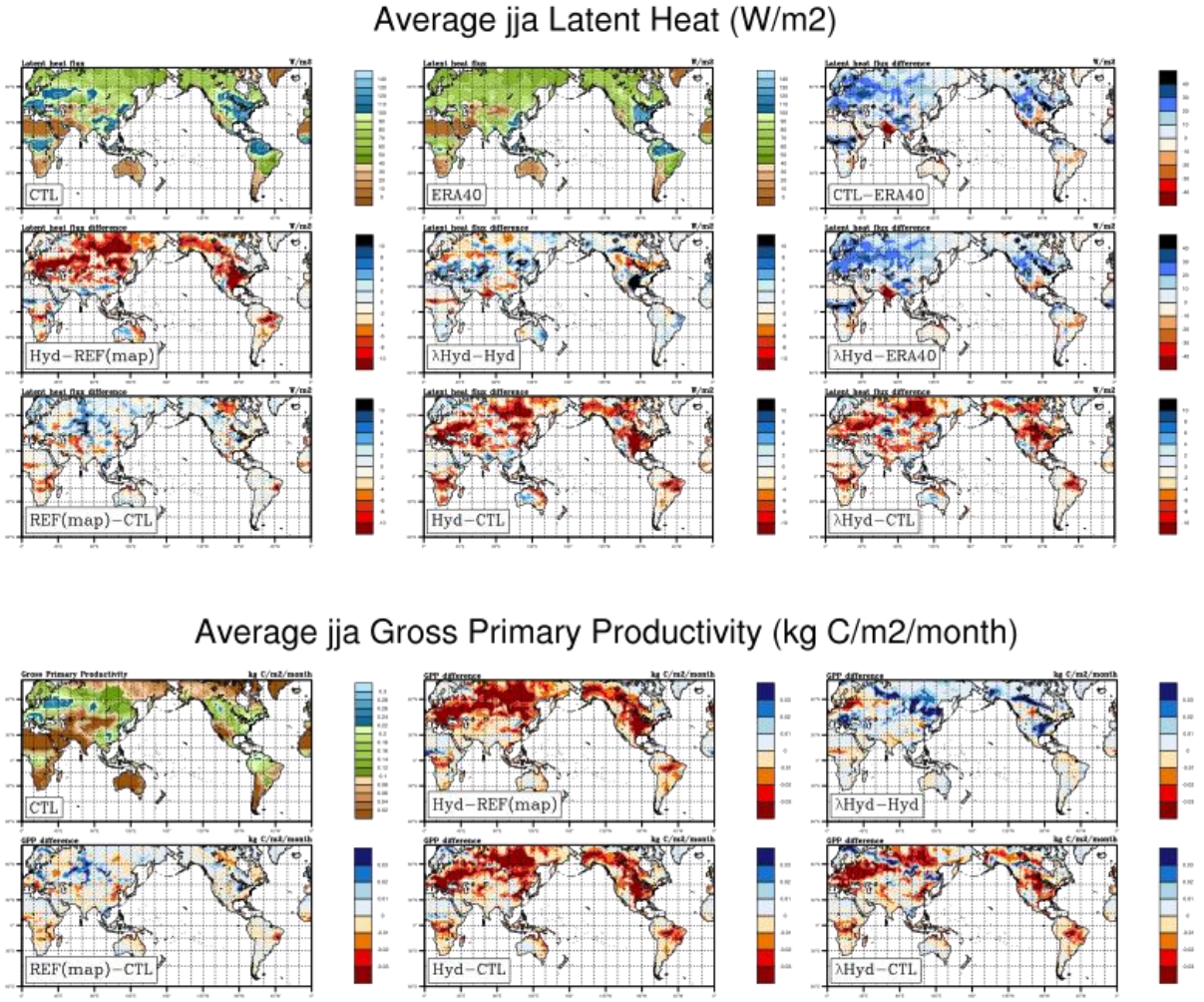

Figure 5. Global maps of latent heat flux (top) and GPP (bottom) from the experiments detailed in Section 2.3. On the top left of each panel, results from the CTL. Also shown are the ERA40 latent heat fields; the additional plots show the differences introduced by each incremental experiment.

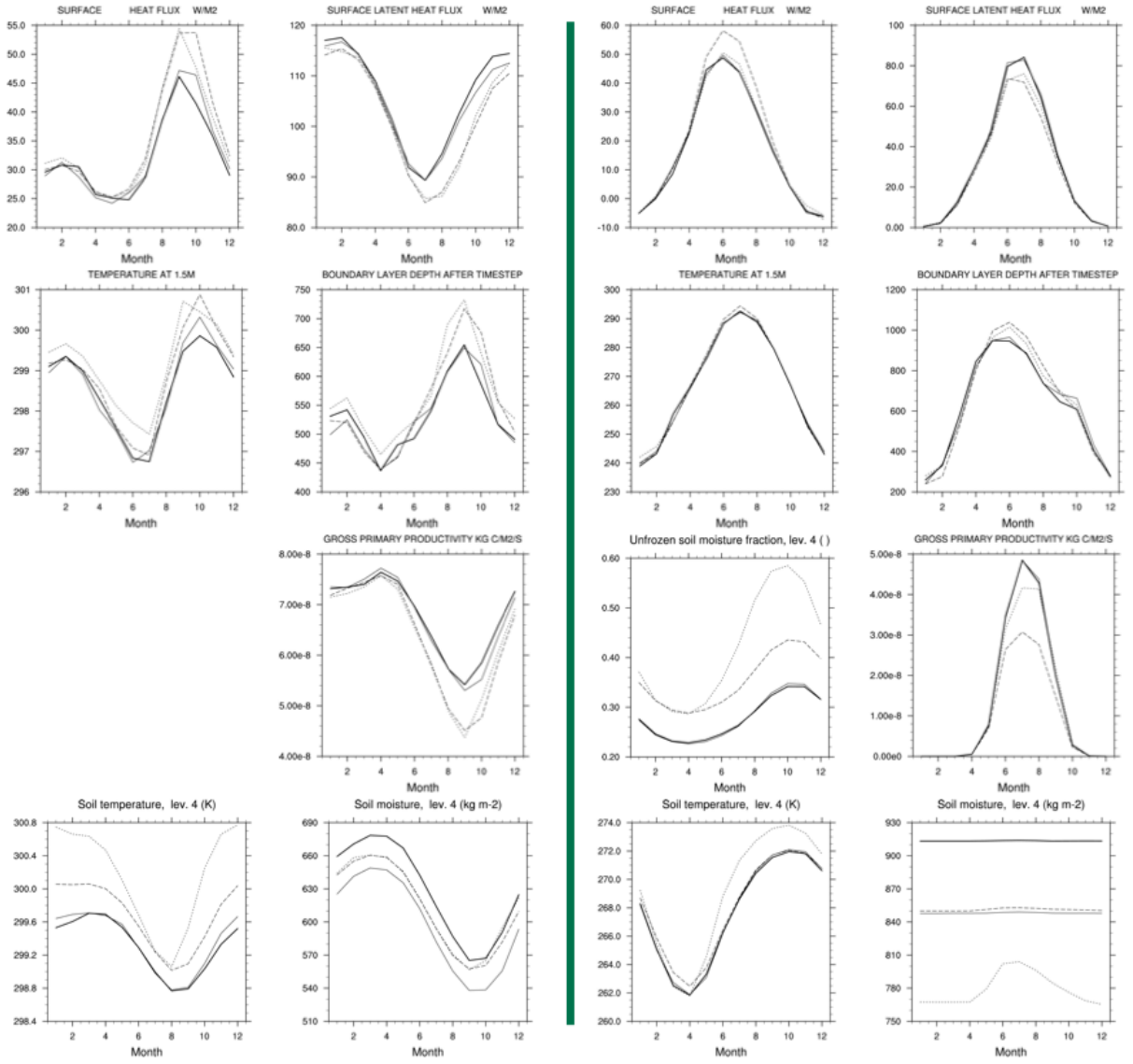

Figure 6. Seasonal variation in key surface (top two panels) and soil (bottom) variables for the GCM simulation runs presented in Section 2.3. Plots are for regional domains over Amazonia on the left-hand panel; for North East Asia on the right-hand panel.

3.3. Monthly anomalies

GCMs disagree on the dynamics of the hydrological cycle, its land surface branch in particular, as well as on the land-atmosphere coupling strength.

Hadley Centre GCMs have the lowest land-atmosphere coupling strength, due to a number of model errors in the formulation of the atmosphere, surface and soils.

We computed monthly anomalies, as deviations from monthly means, for several regional domains worldwide (for a total of 19), targeting two "hot-spot" regions. Two locations are shown, one in the Amazonian forest and the other in the Boreal forest of NE Asia. The results in the Amazon indicate a strengthening of the land surface – atmosphere coupling with the new soil formulation, which is also confirmed in West Equatorial Africa and in Central Africa (compare with map in Figure 5). Results in the Boreal forest of NE Asia indicate that improved thermal exchanges with deeper portions of the soil

strengthen the coupling. This investigation will be expanded into soil moisture – precipitation relations.

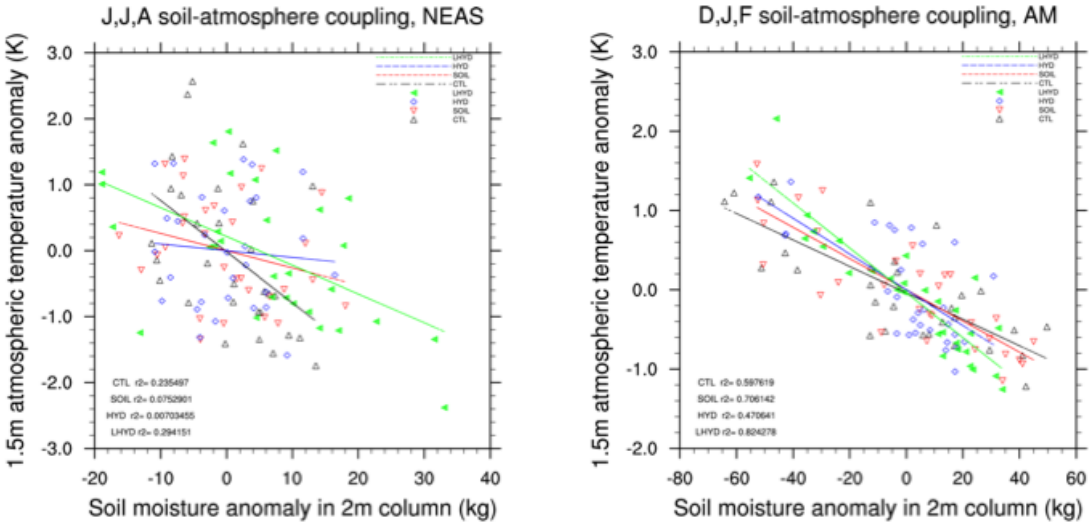

Figure 7. Soil water and surface temperature anomalies over selected regional domains: Amazonia and NE Asia. Monthly deviations for the Amazonian rain season (December, January and February), as well as for the boreal summer in NEAS (June, July and August). 10 years are shown, comprising a total of 30 pairs.

4. References

Cosby BJ, Hornberger GM, Clapp RB and Ginn TR,1984. A statistical exploration of the relationships of soil moisture characteristics to the physical characteristics of soils. Water Resour. Res. 20, 682-690.

Cox PM, Betts RA, Bunton CB, Essery RLH, Rowntree PR, and Smith J, 1999. The impact of new land surface physics on the GCM simulation of climate and climate sensitivity. Clim. Dyn. 15, 183–203.

Dharssi I, Vidale PL, Verhoef A, Macpherson B, Jones C and Best M, 2009. New soil physical properties implemented in the Unified Model at PS18 by UKMO R&D Technical report 528.

Johansen O, 1975. Thermal conductivity of soils. PhD thesis, University of Trondheim, 236 pp.

Johns TC, Durman CF, Banks HT, Roberts MJ et al., 2006. The new Hadley Centre climate model HadGEM1: Evaluation of coupled simulations. J. Climate, 19, 1327-1353.

Koster RD, Dirmeyer PA, Hahmann AN, Ijpelaar R, Tyahla L, Cox P, and Suarez MJ, 2002: Comparing the degree of land–atmosphere interaction in four atmospheric general circulation models. J. Hydrometeor., 3, 363–375.

Lu S, Ren T, Gong Y and Horton R, 2007. An improved model for predicting soil thermal conductivity from water content at room temperature. Soil Sci. Soc. Am J., 71, 8-14.

Verhoef A, Vidale PL, 2009. Influence of soil physical description on key surfaces fluxes and variables predicted by the JULES UK community land surface model. Submitted to Journal of Geophysical Research.